Journal of Advanced Research 42 (2022) 205–219

Contents lists available at ScienceDirect

Journal of Advanced Research

journal homepage: www.elsevier.com/locate/jare

Original Article

SmbHLH60 and SmMYC2 antagonistically regulate phenolic acids and anthocyanins biosynthesis in *Salvia miltiorrhiza*

Shucan Liu [a,b,1], Yao Wang [b,c,1], Min Shi [b], Itay Maoz [d], Xiankui Gao [b], Meihong Sun [c], Tingpan Yuan [c], Kunlun Li [b], Wei Zhou [b], Xinhong Guo [a,*], Guoyin Kai [b,*]

[a] College of Biology, Hunan University, Changsha, Hunan 410082, PR China
[b] Laboratory of Medicinal Plant Biotechnology, School of Pharmaceutical Sciences, Zhejiang Chinese Medical University, Hangzhou, Zhejiang 310053, PR China
[c] Institute of Plant Biotechnology, School of Life Sciences, Shanghai Normal University, Shanghai 200234, PR China
[d] Department of Postharvest Science, Agricultural Research Organization, The Volcani Center, HaMaccabim Rd 68, POB 15159, Rishon LeZion 7528809, Israel

HIGHLIGHTS

- *SmbHLH60* is one of the most significantly down-regulated bHLH genes induced by MeJA.
- Phenolic acids and anthocyanins were obviously reduced in *SmbHLH60*-OE hairy roots whereas phenolic acids and anthocyanins were significantly increased in *SmbHLH60*-CRISPR hairy roots.
- SmbHLH60 negatively regulates phenolic acid biosynthesis mainly via *SmTAT1* gene.
- SmbHLH60 negatively regulates anthocyanin biosynthesis mainly via *SmDRF* gene.
- SmbHLH60 works with SmMYC2 in an antagonistic manner in phenolic acid biosynthesis.

GRAPHICAL ABSTRACT

We discovered that a new transcription factor SmbHLH60 repressed the biosynthesis of phenolic acids and anthocyanins in *S. miltiorrhiza* through transcriptional inhibition of *SmTAT1* and *SmDFR*. In addition, SmbHLH60 and SmMYC2 formed a heterodimer to antagonistically regulate phenolic acids and anthocyanins biosynthesis.

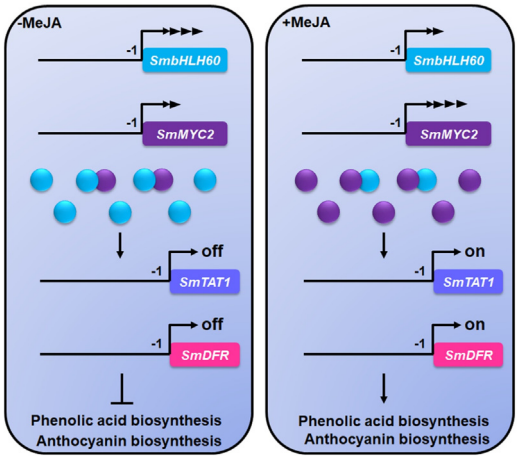

ARTICLE INFO

Article history:
Received 16 August 2021
Revised 3 January 2022
Accepted 12 February 2022
Available online 17 February 2022

ABSTRACT

Introduction: Salvia miltiorrhiza is a renowned traditional Chinese medicinal plant with extremely high medicinal value, especially for cardiovascular and cerebrovascular diseases. The jasmonic acid (JA) signaling pathway plays an important role in the improved biosynthesis of secondary metabolites, which is mediated by a major transcriptional regulator, MYC2. However, the JA regulatory mechanism of secondary metabolites biosynthesis in *S. miltiorrhiza* is still largely unknown.

Peer review under responsibility of Cairo University.
* Corresponding authors.
E-mail addresses: gxh@hnu.edu.cn (X. Guo), kaiguoyin@163.com (G. Kai).
[1] These authors contribute equally.

https://doi.org/10.1016/j.jare.2022.02.005

Keywords:
Salvia miltiorrhiza
SmbHLH60
SmMYC2
Phenolic acid
Anthocyanin
Antagonistic regulation

Objectives: Our work focuses on the dissection of the molecular mechanism of transcriptional regulation in MeJA-mediated biosynthesis of medicinal components of *S. miltiorrhiza*. We examined the role of MeJA-responsive bHLH transcription factors (TFs) in improving bioactive secondary metabolites accumulation in *S. miltiorrhiza*.
Methods: Hairy root transformation based on CRISPR/Cas9 technique was used to decipher gene function (s). Changes in the content of phenolic acids were evaluated by HPLC. Y1H, EMSA and dual-LUC assays were employed to analyze the molecular mechanism of SmbHLH60 in the regulation on the biosynthesis of phenolic acids and anthocyanins. Y2H, BiFC and pull-down affinity assays were used to corroborate the interaction between SmbHLH60 and SmMYC2.
Results: Being one of the most significantly negatively regulated bHLH genes by MeJA, a new transcription factor SmbHLH60 was discovered and characterized. Over-expression of *SmbHLH60* resulted in significant inhibition of phenolic acid and anthocyanin biosynthesis in *S. miltiorrhiza* by transcriptionally repressing of target genes such as *SmTAT1* and *SmDFR*, whereas CRISPR/Cas9-generated knockout of *SmbHLH60* resulted in the opposite effect. In addition, SmbHLH60 and SmMYC2 formed a heterodimer to antagonistically regulate phenolic acid and anthocyanin biosynthesis.
Conclusion: Our results clarified that SmbHLH60 is a negative regulator on the biosynthesis of phenolic acids and anthocyanins. SmbHLH60 competed with SmMYC2 in an antagonistic manner, providing new insights for the molecular mechanism of MeJA-mediated regulation on the biosynthesis of secondary metabolites in *S. miltiorrhiza*.

Introduction

Salvia miltiorrhiza, *Lamiaceae* family, is a medicinal herb widely used in Chinese medicine for treatments of cardiovascular and cerebrovascular diseases [1–5]. The composition and concentration of phenolic acids and liposoluble tanshinones are associated with their health-promoting properties [1,3,6]. Caffeic acid (CA), salvianolic acid B (SAB), salvianolic acid A (SAA) and rosmarinic acid (RA) are the main bioactive phenolic acids identified and reported to have anti-oxidant, anti-inflammatory, anti-atherosclerosis, anti-tumor, and anti-diabetic activities [7–9]. High economic value and increasing market demands for enhanced content of phenolic acids derive current researches focus on the regulation of phenolic acid biosynthesis pathways [3,10–12].

In plants, the phenolic acid biosynthesis pathway has been extensively studied and in *S. miltiorrhiza* two upstream pathways have been characterized: the phenylpropane metabolic pathway and the tyrosine-derived metabolic pathway (Fig. S1) [3,12–14]. In the phenylpropane metabolic pathway, L-phenylalanine is sequentially metabolized by phenylalanine ammonia-lyase (PAL), cinnamic acid 4-hydroxylase (C4H) and 4-coumarate: CoA ligase (4CL) to generate one of the precursors, 4-coumaroyl-CoA [15–17]. In parallel, tyrosine conversion is catalyzed by tyrosine aminotransferase (TAT), 4-hydroxyphenylpyruvate reductase (HPPR) and additional uncharacterized enzymatic steps to form the other precursor, 3,4-dihydroxyphenyllactic acid [15,18]. Subsequently, the two precursors will be used to generate rosmarinic acid catalyzed by rosmarinic acid synthase (RAS) and cytochrome P450-dependent monooxygenase (CYP98A14). The formation of additional phenolic acids by these two precursors may occur by yet unknown step(s) [10,13,19].

4-coumaroyl-CoA is an important precursor in the phenylpropanoid pathway taking part in the production of numerous phenylpropanoids including anthocyanins [3]. The latter is extremely important secondary metabolites, widely distributed among higher plants, serve as important natural pigments and have strong antioxidant activity, and are therefore beneficial for the human diet [20,21]. So far, a major part of the anthocyanin biosynthesis pathway in *S. miltiorrhiza* has been characterized including chalcone synthase (SmCHS), chalcone isomerase (SmCHI), flavone synthase (SmFNS), flavanone 3-hydroxylase (SmF3H), flavonoid 3′-hydroxylase (SmF3′H), flavonoid 3′,5′-hydroxylase (SmF3′5′H), flavonol synthase (SmFLS), dihydroflavonol 4-reductase (SmDFR), and anthocyanidin synthase (SmANS) [12,22]. However, only a few works studied the regulation mechanism of anthocyanins in *S. miltiorrhiza*.

Many elicitors including gibberellins (GAs), methyl jasmonate (MeJA), abscisic acid (ABA), salicylic acid (SA), yeast extract (YE), Ag^+, nitric oxide (NO), and hydrogen peroxide (H_2O_2) have been proven to increase the phenolic acids accumulation [16,23–25]. In addition, MeJA has been used to increase the content of anthocyanins [3,20,26]. However, the mechanism in which MeJA-induced phenolic acid and anthocyanin regulation in *S. miltiorrhiza* is still largely unknown.

The basic helix-loop-helix (bHLH) TF family plays an extremely important role in secondary metabolism regulation [27–29]. It was also shown that bHLHs can bind to specific promoter regions in their targeted genes, such as E-box (CANNTG) or G-box (CACGTG) [8,30–32]. Currently, 127 bHLH TFs were found in *S. miltiorrhiza* by genome mining [4,33], some of which were discovered to be involved in the regulation of secondary metabolism. For example, SmbHLH3 negatively regulates phenolic acid biosynthesis by modulating *SmTAT1* and *SmHPPR1* [34]. RA, SAB and CA levels were increased by 2.87, 4.00 and 5.99 times, respectively, as compared to the control in SmbHLH148 [35]. SmbHLH10 increased the accumulation of tanshinone in the roots of *S. miltiorrhiza* [36]. SmbHLH92 and SmbHLH37 have been confirmed to negatively regulate phenolic acids biosynthesis pathways while SmbHLH51 functions as a positive regulator [8,37,38]. SAB biosynthesis, in *S. miltiorrhiza*, triggered by MeJA is also regulated by SmbHLH53 presumably with a dual-role [14]. MYELOCYTOMATOSISs (MYCs), another type of bHLH TFs, were also shown to take a central role in secondary metabolites regulation. For example, AaMYC2, a jasmonate-responsive TF, positively regulates artemisinin biosynthesis in *Artemisia annua* [39]. In *Catharanthus roseus*, CrMYC2 has been proved to be essential for the accumulation of alkaloids [40]. In *S. miltiorrhiza*, SmMYC2 plays a role as a core transcription factor in the MeJA-mediated phenolic acid secondary metabolism signaling pathway by actively binding to *SmPAL1*, *SmTAT1* and *SmCYP98A14* promoters altering their expression, leading to the accumulation of phenolic acids [37,41]. Still, in *S. miltiorrhiza,* the mechanism in which SmMYC2 regulates MeJA-mediated phenolic acid and anthocyanin biosynthesis is not fully understood. Our data suggest that by forming a heterodimer, SmbHLH60 and SmMYC2 antagonistically regulate anthocyanin and phenolic acid biosynthesis. Our new findings reveal the molecular regulation

mechanism of SmbHLH60 and SmMYC2 and elucidate the MeJA-mediated regulation of secondary metabolites regulation in *S. miltiorrhiza*.

Materials and methods

Plant materials

S. miltiorrhiza seedlings were grown in the greenhouse of Zhejiang Chinese Medical University. *S. miltiorrhiza* seedlings were cultured on Murashige and Skoog (MS) medium at 25 °C, which were lighted for 16 h and dark for 8 h. *Nicotiana benthamiana* was cultivated in a greenhouse at 25 °C, under the same conditions as *S. miltiorrhiza*. *S. miltiorrhiza* hairy roots were grown on 1/2 MS solid medium and cultured in the dark in a greenhouse at 25 °C. For culture in a flask, the hairy roots were cultured in 100 mL 1/2 MS liquid medium at 120 rpm for 50 days in the dark.

Isolation and characterization of SmbHLH60

SmbHLH60 was found to be one of the most significantly down-regulated bHLH genes in RNA-Seq data, and the full-length cDNA was amplified using specific primers (Table S1). ClustalX and MEGA 6.0 software were used for sequence alignment and phylogenetic tree analysis. The phylogenetic tree was constructed based on the amino acid sequence with the neighbor-joining method and then optimized with the iTOL tool. All protein sequences including SibHLH130 (XP_011087339.1), SibHLH130-like (XP_011093536.1), PjbHLH130 (GFQ08151.1), OebHLH130-like (XP_022896111.1) used in multiple sequence alignment were download from NCBI database.

Gene expression profile assay

For RNA isolation, different tissues of one-year-old *S. miltiorrhiza* plants, including roots, lateral roots, stems, xylems, phloems, leaves and young leaves were collected and performed using the Tiangen Plant RNA Extraction Kit. Followed by reverse transcription and qRT-PCR for *SmbHLH60* gene detection, *SmActin* was used as an internal reference. Exogenous plant hormones including 100 μM methyl jasmonate (MeJA) was used to spray one-month-old *S. miltiorrhiza* seedlings and sampled at 0, 1, 2, 4, 6, 8, 12, 24 h after treatment for RNA extraction, followed by reverse transcription and qRT-PCR to detect *SmbHLH60* gene expression. The relative quantitative analysis method ($2^{-\Delta\Delta CT}$) was used to calculate the relative gene expression, and *SmActin* was used as the internal reference gene and all experiments were repeated with more than three biological replicates.

Subcellular localization of SmbHLH60

To determine the subcellular localization of SmbHLH60, the open reading frame (ORF) of *SmbHLH60* was cloned and constructed into the pHB-YFP vector driven by the CaMV 35S promoter to form the SmbHLH60-YFP fusion protein (Fig. S2B). The negative control was performed by an empty pHB-YFP vector. The fusion vector was transformed into *Agrobacterium tumefaciens* GV3101 strain. Then the transformed GV3101 was injected into five-week-old *N. benthamiana* leaves while pHB-YFP was used as a negative control. To confirm the position of the nucleus, 10 mg/mL 4′,6-diamidino-2-phenylindole dihydrochloride (DAPI) solution was injected into *N. benthamiana* leaves 4 h before observing the fluorescence signal. Then the fluorescence signal was observed by laser confocal microscope (Zeiss, Germany) under the excitation of 405 nm and 488 nm laser. All experiments were repeated with more than three biological replicates.

Generating S. miltiorrhiza hairy roots

The complete ORF of *SmbHLH60* was cloned into the pCAMBIA2300^{+} vector containing the CaMV 35S promoter to form the pCAMBIA2300^{+}-*SmbHLH60* recombinant vector (Fig. S2A). For the knockout vector, sgRNA was designed according to the 5′-G-19base-NGG-3' principle, which was constructed on the pCAMBIA2300^{+} vector (Fig. S2A). *SmbHLH60* sgRNA was driven by the AtU6 promoter, and hSpCas9 was by the CaMV 35S promoter with pCAMBIA2300^{+} serving as a control vector. The above vectors were transformed into C58C1 and then used to infect *S. miltiorrhiza* for hairy roots. The hairy root DNA was extracted by the CTAB method and the positive clones were identified with specific primers (Table S1). All experiments were repeated with three biological replicates.

Quantitative real-time PCR (qRT-PCR)

Tissues including taproots, lateral roots, xylems, phloems, stems, leaves, and tender leaves of *S. miltiorrhiza* were collected and ground into a powder with liquid nitrogen to extract total RNA and follow the steps in the Tiangen plant total RNA extraction kit. The qRT-PCR experiments were used to detect the results with Thermo Fisher quantitative master mix and the Applied Biosystem Step One Real-Time PCR System (Applied Biosystems, USA) and the *SmActin* was used as an internal control [42]. All experiments had three biological replicates.

Measuring the accumulation of phenolic acids and anthocyanins in hairy roots

0.1 g of dried hairy root powder was weighed for phenolic acid extraction with 80% ethanol solution (4:1, v/v), and ultrasonic extraction was performed for 30 min. The extract was dissolved in 2 mL of distilled water after vacuum rotary steaming. HPLC was used to detect each component in the phenolic acid extract, and the content was calculated by substituting it into the standard curve. In addition, 0.02 g of dried hairy root powder was weighed and mixed in 1 mL of 1% (v/v) hydrochloric acid methanol solution (hydrochloric acid: methanol = 1:99), at 100 rpm, 20 °C overnight for total anthocyanin extraction. Then samples were centrifugated at 12,000 rpm and the supernatant was taken for further analysis. Samples were mixed similar volume of chloroform and the absorbance of the extract at 530 nm and 657 nm wavelengths were detected by spectrophotometry. Anthocyanin content Q (anthocyanin) = (A530-0.25 × A657) × M^{-1}, and M is the dry weight of plant tissue. All measurements were carried out in three biological replicates.

Yeast one-hybrid assay (Y1H)

The complete *SmbHLH60* ORF sequence was constructed on the pB42AD vector to form a recombinant vector, and the E/G-box in the promoters of key genes of phenolic acid and anthocyanin biosynthesis were constructed on the pLacZ2u vector. The recombinant plasmid was co-transformed into yeast strain EGY48, followed cultured on SD/-Ura/-Trp medium for 48 h. Then the positive colony was picked and tested for growth of monoclonal strains on SD/-Ura/-Trp/Raf/Gal medium with X-gal for 48 h. Empty vectors pB42AD and pLacZ2u were used as negative controls. We performed the Y1H experiment more than three biological replicates.

Electrophoretic mobility shift assay (EMSA)

The ORF of *SmbHLH60* was inserted into the vector pCold-His. Recombinant protein SmbHLH60-His was expressed in *E. coli* BL21 (DE3) and purified using a protein purification kit with a His-tag, which was purchased from Shanghai Sangon Co., Ltd. Probe fragments from the promoter of *SmTAT1* and *SmDFR* were synthesized by Shanghai Sangon Co., Ltd. The 5 × EMSA binding buffer was purchased from Beyotime Biotechnology Co., Ltd. (Shanghai, China), and the chemiluminescence detection kit was purchased from Thermo Fisher Scientific (Shanghai, China), and the fluorescence was detected using a C300 image scanner (Azure Biosystems, USA). SmbHLH60-His purified protein was combined with probes of *SmTAT1pro* and *SmDFRpro* by adding 5 × binding buffer (Beyotime Biotechnology Co., Ltd.) at 25 °C for 25 min. Then follow the previously reported method [12,42]. EMSA experiment was repeated with three biological replicates.

Dual-luciferase assay (dual-LUC)

Promoters about 2000 bp of all key enzyme genes involved in phenolic acid and anthocyanin biosynthesis were constructed to pGreen0800-LUC vector. The recombinant vector was then transferred to *A. tumefaciens* GV3101. The *N. benthamiana* was then transformed instantaneously by infiltrating the *Agrobacterium* mixture into the back of the leaves. After 48 h, samples were taken from the infected site, and the extract was detected using a dual-luciferase reporter analysis system (Promega, Madison, USA), and the fluorescence values were detected. All dual-LUC experiments were repeated for more than three biological replicates.

Bimolecular fluorescent complementary assay (BiFC)

To verify the interaction between SmbHLH60 and SmMYC2, the full-length ORF of *SmbHLH60* and *SmMYC2* were constructed on pXY106-nYFP and pXY104-cYFP, respectively, and then transformed into *A. tumefaciens* GV3101. The resuspended *Agrobacteria* were mixed and injected into *N. benthamiana* leaves for transient expression. Then *N. benthamiana* plants were placed in a greenhouse at 26 °C for 48 h, and the yellow fluorescence was observed by laser confocal microscope (Zeiss, Germany) under the excitation of 488 nm lasers previously described [3,12]. This experiment was repeated with three replicates.

GST pull-down assay

The complete ORFs of *SmbHLH60* and *SmMYC2* were respectively constructed on the pCold-His vector and pGEX-4T-1 vector, which were transformed into *E. coli* BL21 (DE3) for protein expression, using His-tag and GST-tag protein purification kit (Shanghai Sangon Co., Ltd) for purification, respectively. SmMYC2-GST was incubated with GST magnetic beads (Shanghai Sangon Co., Ltd) at 26 °C for 30 min to form a GST-target protein complex. Subsequently, SmbHLH60-His recombinant protein was added for the binding reaction at 4 °C overnight. After 3000 rpm centrifugation, the supernatant was aspirated and used for input detection by anti-GST and anti-His. Then, the magnetic beads were washed 3 times with wash buffer, the supernatant was discarded. Finally, the elution buffer was added to elute the protein, which was taken for electrophoresis and western blot detection by anti-His. This experiment had three biological replicates.

Results

SmbHLH60 expression pattern analysis

SmbHLH60 was found to be one of the most significantly down-regulated bHLH genes in MeJA-mediated RNA-Seq data (Fig. 1A). To examine the involvement of *SmbHLH60* in the MeJA signaling pathway, exogenous MeJA was applied to the whole plant, and the expression of *SmbHLH60* was examined by qRT-PCR. *SmbHLH60* expression was significantly decreased in MeJA-treated samples as compared to control (0 h) from 1 h, reaching the lowest levels at 6 h (Fig. 1B). These results showed good accordance with our previous RNA-seq data. In addition, *SmbHLH60* showed an opposite expression pattern with *SmMYC2* and genes involved in phenolic acid biosynthesis such as *SmPAL1*, *SmC4H*, *SmTAT1*, *SmHPPR*, *SmRAS* and *SmCYP98A14* after MeJA treatment (Fig. 1A). Meanwhile, we analyzed the expression patterns of *SmbHLH60* and the previously characterized *SmbHLHs* under MeJA treatment. We found that the expression of *SmbHLH92*, a negative regulator in the biosynthesis of phenolic acid, decreased in MeJA-mediated RNA-seq data (Fig. S5), which showed a similar expression pattern to *SmbHLH60*. Therefore, we speculated that SmbHLH60 may participate in the negative regulation of phenolic acid. Total phenolic acid accumulation in the leaf of *S. miltiorrhiza* was the highest among the three tissues (root, leaf and stem) (Fig. S6). Tissue expression profile showed that *SmbHLH60* expressed the highest in leaf, especially in young leaf (Fig. 1C). Meanwhile, *SmMYC2* was found to have the highest expression in the leaf [43]. These results support that SmbHLH60 might participate in the regulation of phenolic acids. Therefore, we focused on the research of *SmbHLH60*.

Isolation and characterization of SmbHLH60

*SmbHLH*60 sequence contained an 1185 bp of an open reading frame, encoding a 394 amino acids protein with a size prediction of 43.58 kDa. To explore the evolutionary relationship between SmbHLH60 and 167 bHLH TFs in *Arabidopsis thaliana*, the phylogenetic tree was constructed, which showed that SmbHLH60 was high homology with AtbHLH130 (Fig. S3). The latter is known as FLOWERING BHLH4 (FBH4) and it was reported to activate CONSTANS (CO) with FBH1, FBH2, and FBH3 redundantly as part of the flowering regulatory mechanism in *A. thaliana* [43]. The result of BLAST-Protein (BLASTP) analysis showed that SmbHLH60 has the highest identity (60.58%) to *Sesamum indicum* bHLH130. All proteins, including SibHLH130-like, PjbHLH130, OebHLH130-like contained the basic helix-loop-helix conserved domain at the C-terminus (Fig. 2A). Subcellular localization assay was used to explore the location of SmbHLH60 in cells. SmbHLH60-YFP fluorescence was observed in the nucleus using a laser confocal microscope, while the YFP signal of pHB-YFP was distributed in the cell nucleus and cytoplasm, and DAPI appeared in the nucleus (Fig. 2B).

Generation of SmbHLH60-overexpression and SmbHLH60-CRISPR hairy roots

To decipher the role of *SmbHLH60* in phenolic acid and anthocyanin accumulation, transgenic lines were generated. Recombinant vectors pCAMBIA2300^{+}-*SmbHLH60* and pCAMBIA2300^{+}-*SmbHLH60*-CRISPR/Cas9 were separately transfected into the modified *A. tumefaciens* C58C1 harboring *A. rhizogenes* A4 Ri plasmid. For infecting explants of *S. miltiorrhiza* to obtain genetically modified hairy roots. Fig. S4 showed the results that the positive *SmbHLH60*-OE lines were identified with primer in Table S1. EV means hairy roots which derive from infecting with *A. rhizogenes*

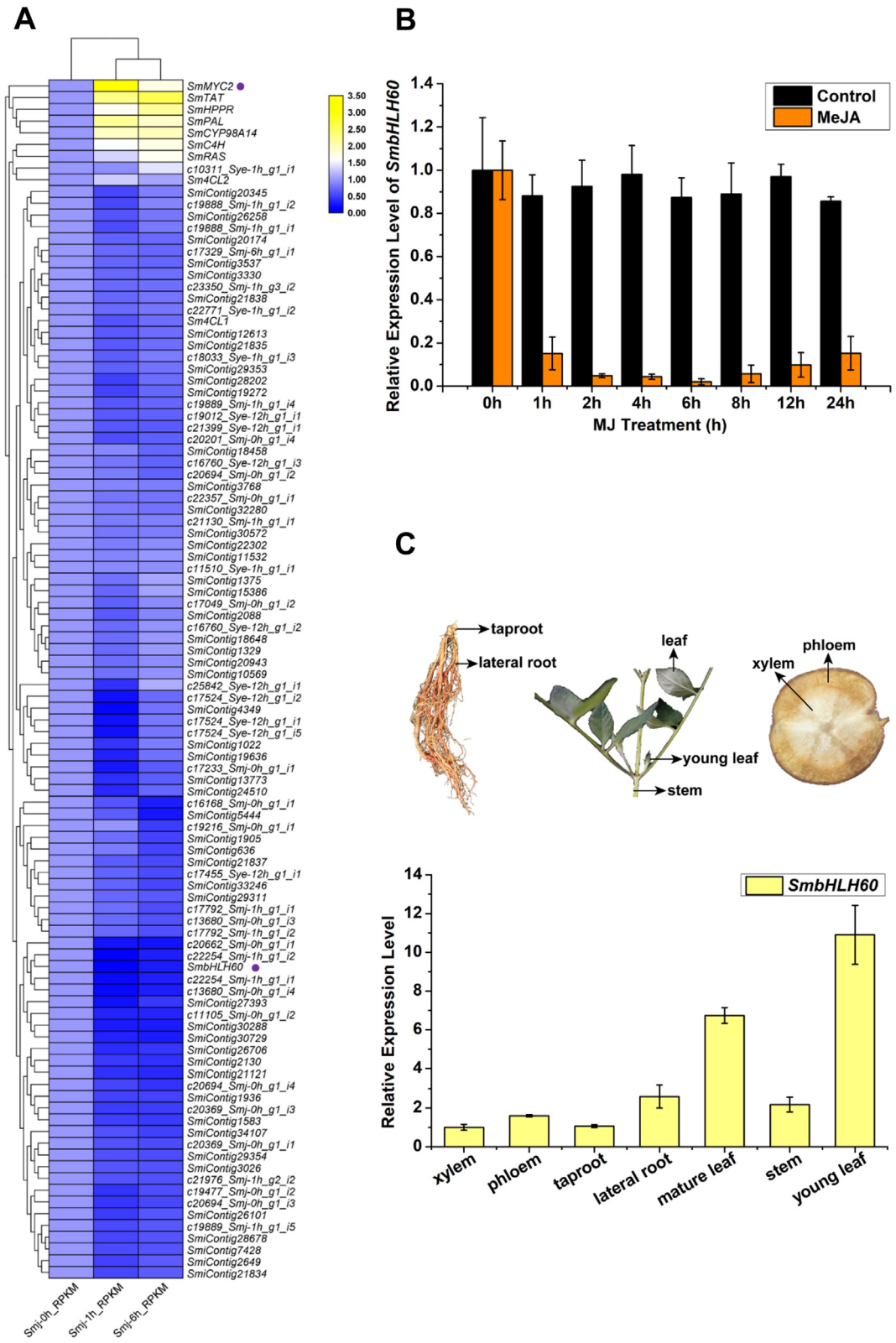

Fig. 1. Expression profiles analysis of *SmbHLH60*. (A). The analysis of *SmbHLH60* expression pattern in MeJA-induced transcriptome library at 1 h and 6 h. The heat map was produced using TBtools. The yellow color indicated high expression levels, and the blue color indicated low expression levels. A total of 89 bHLH TFs showed decreased expression after MeJA treatment revealed in the transcriptome library. The expression of *SmbHLH60* decrease obviously after MeJA treatment at 1 h (B). The effect of exogenous MeJA on the expression of *SmbHLH60*. The expression of *SmbHLH60* was detected under MJ treatment for 0 h, 1 h, 2 h, 4 h, 6 h, 8 h, 12 h, 24 h. *SmbHLH60* was drastically decreased under the regulation of MeJA in the whole plant. (C). *SmbHLH60* gene expressions in different tissues of *S. miltiorrhiza*. The transcription level of *SmbHLH60* was detected in the xylem, phloem, taproot, lateral root, mature leaf, steam and young leaf respectively. All experiments were repeated three times, and the error bars represented the standard deviation of the three replicates. (For interpretation of the references to color in this figure legend, the reader is referred to the web version of this article.)

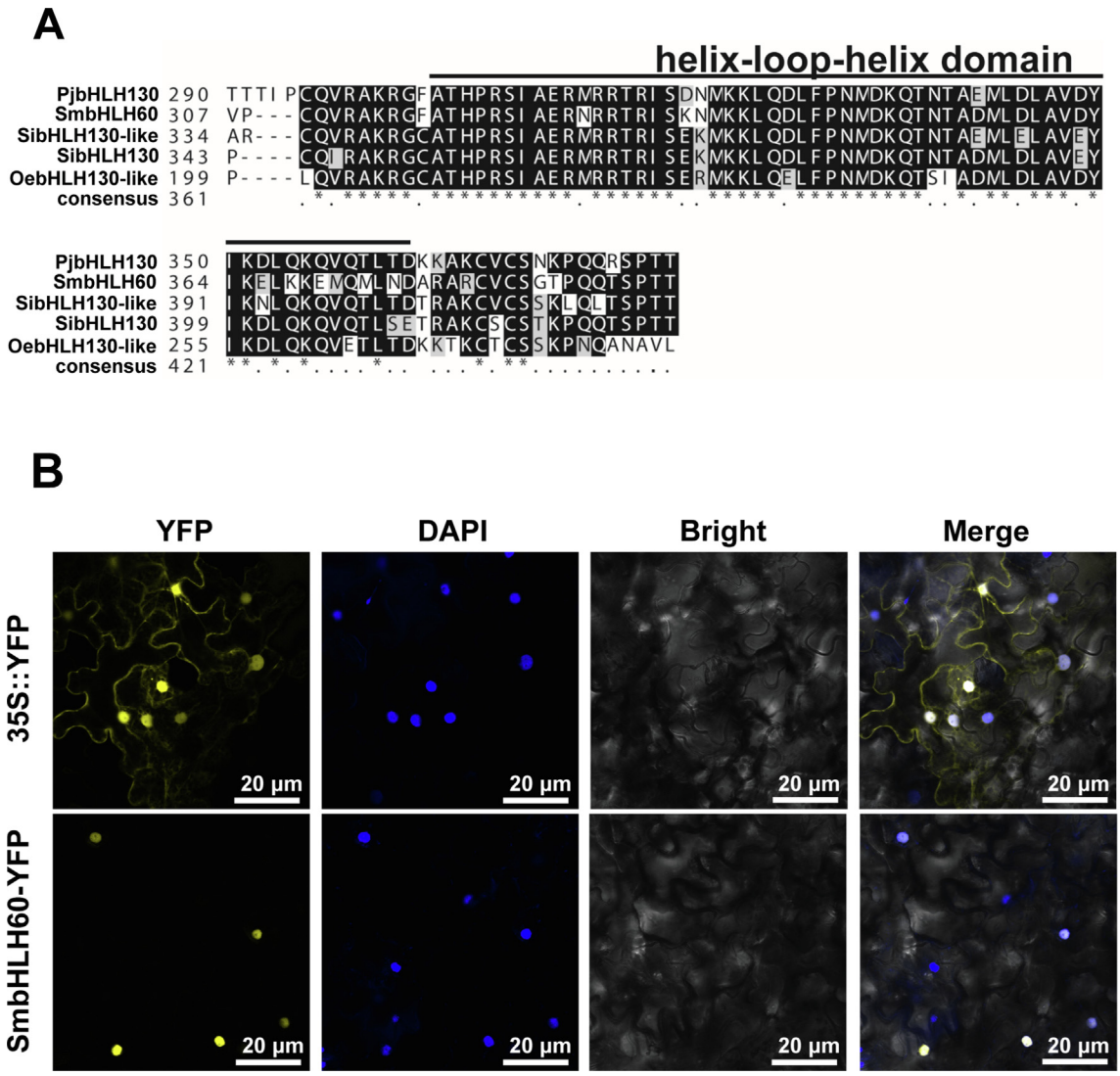

Fig. 2. Characterization and subcellular localization of SmbHLH60. (A). ClustalX was performed for multiple sequence alignment. Multiple amino acid sequence alignments of bHLH TFs including SibHLH130 (XP_011087339.1), PjbHLH130 (GFQ08151.1), OsbHLH130-like (XP_022896111.1) and SibHLH130-like (XP_011093536.1). (B). Subcellular localization of SmbHLH60 in *N. benthamiana* leaf epidermal cells. YFP fluorescence and DAPI signals were observed at 488 nm and 405 nm.

C58C1 containing empty vector (pCAMBIA2300^{+}) plasmid, which was used as a negative control. The CRISPR/Cas9 knockout lines used target sequence-specific primers to amplify about 400 bp sequence for sequence determination. The sequencing results and sequencing diagrams were shown in Fig. 3C-D, and the TGG was the PAM sequence. Four *SmbHLH60* overexpression (*SmbHLH60*-OE) and four CRISPR/Cas9 knockout lines (*SmbHLH60*-CRISPR) were used for further analysis (Fig. 3A). In *SmbHLH60*-OE lines, the expression levels of *SmbHLH60* were significantly higher as compared to the control. Conversely, expression levels of *SmbHLH60* were much lower in the knockout lines as compared to the control (Fig. 3B).

SmbHLH60 reduces the phenolic acid accumulation

Total polyphenol content was determined using Folin-Phenol reagent was the highest in the knockout lines, then in the control, and the lowest levels were detected in the *SmbHLH60* overexpression hairy root lines (Fig. 4A). HPLC analysis confirmed our results with total phenolic acids (TS) of 32.77 ± 1.75 mg/g in the knockout lines, significantly higher than the control line with 22.07 ± 2.55 mg/g, while the TS content in *SmbHLH60* overexpression hairy roots was 12.88 ± 3.21 mg/g significantly lower than the control line (Fig. 4B). In accordance with our chemical profiling, the expression level of genes involved in the biosynthesis of phenolic acid *SmPAL1*, *SmC4H1*, *Sm4CL2*, *SmTAT1*, *SmHPPR1*, *SmRAS1* and *SmCYP98A14* were significantly higher in the *SmbHLH60*-CRISPR lines as compared to the control. The expression levels in the *SmbHLH60*-OE lines were significantly lower as compared to the control line (Fig. 4C).

SmbHLH60 negatively regulates anthocyanin biosynthesis

The initial steps of the phenylpropanoid pathway provide the precursors for the biosynthesis of phenolic acids and anthocyanins [3]. Total anthocyanin extracts from hairy roots of different lines exhibited inconsistent colors (Fig. 5A). Therefore, we examined if the effect on color accumulation is directly or indirectly related to the anthocyanin biosynthetic pathway. In the *SmbHLH60*-CRISPR lines, the total anthocyanins were significantly increased, about twice the control. In the *SmbHLH60*-OE lines, the anthocyanin content was significantly reduced, which was about 42% lower than the control (Fig. 5B). Expression of genes involved in the biosynthesis of anthocyanins including *SmCHS*, *SmFLS*, *SmF3H*,

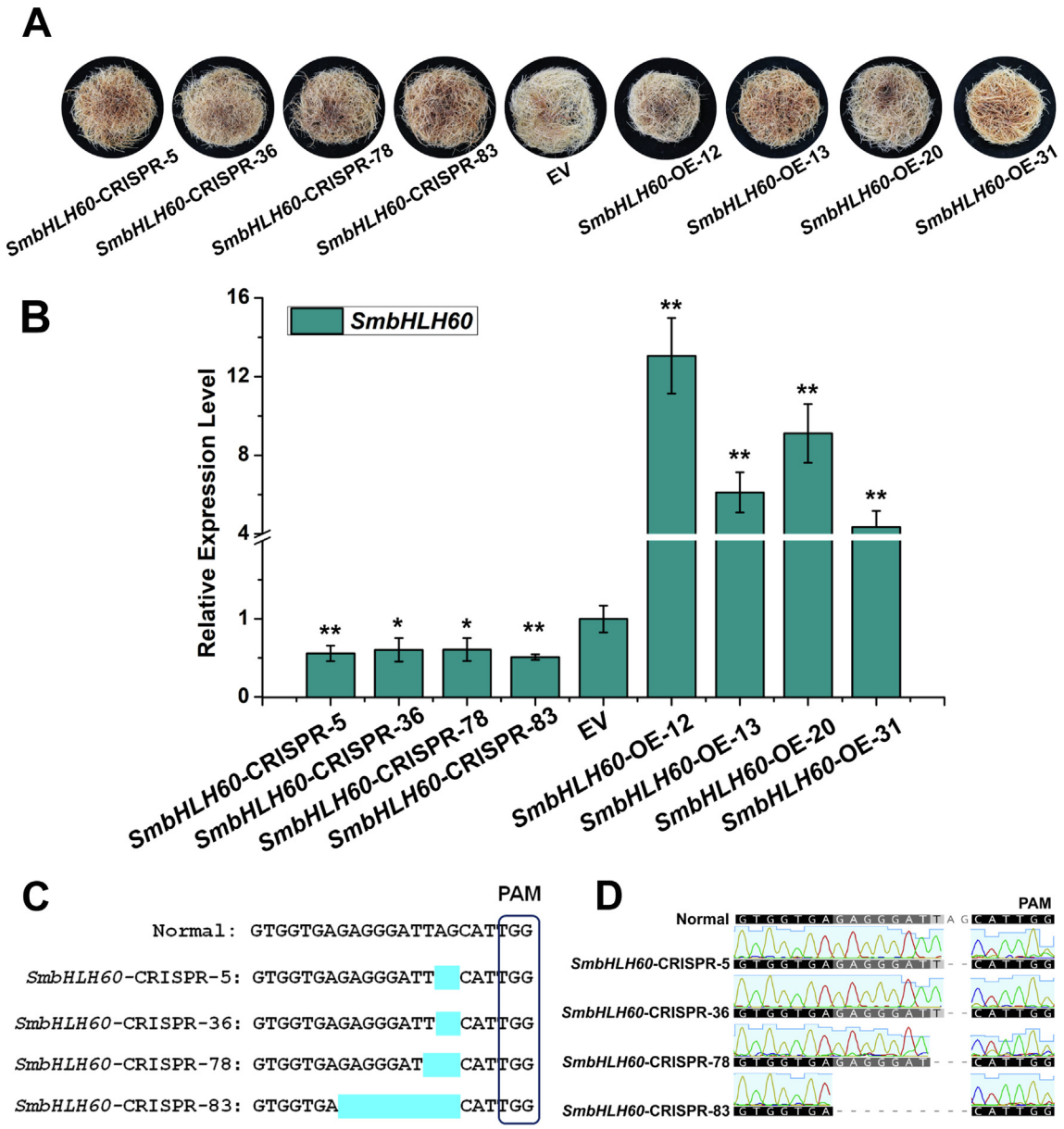

Fig. 3. Generation of transgenic hairy roots. (A). Hairy roots were cultured for 50 days in 1/2MS. Four knockout lines and four overexpression lines were used for cultivation and subsequent experiments. (B). Transcript-level expression of *SmbHLH60* in *SmbHLH60*-CRISPR lines and *SmbHLH60*-OE lines were tested by qRT-PCR and error bars represented the standard deviation of three biological replicates (*, $p < 0.05$; **, $p < 0.01$). (C-D). CRISPR/Cas9 system knocks out hairy root. TGG was the PAM sequence. After being edited with CRISPR/Cas9 system, line 5 and line 36 lacked 2 bases, line 78 lacked 3 bases, and line 83 lacked 10 bases.

SmF3′H, *SmF3′5′H*, *SmANS* and *SmDFR* was significantly higher in the *SmbHLH60*-CRISPR lines as compared to the control, while in the latter it was significantly higher as compared to the *SmbHLH60*-OE lines (Fig. 5C).

SmbHLH60 binds and transcriptionally inhibits the promoters of SmTAT1 and SmDFR

SmbHLH60 caused a decrease in phenolic acid and anthocyanin, so we selected 11 genes (7 key enzyme genes of phenolic acid biosynthesis and 4 key enzyme genes of anthocyanin biosynthesis) whose transcription level decreased significantly in the *SmbHLH60*-OE lines and increased in the *SmbHLH60*-CRISPR lines for dual-LUC experiments. The results showed that *SmTAT1*, *SmPAL1*, *SmRAS1* (phenolic acid biosynthesis pathway) and *SmDFR* (anthocyanin biosynthesis pathway) were significantly transcriptionally repressed by *SmbHLH60* (Fig. 6A-B, S7). Further investigation showed that SmbHLH60 only bound to the G-box element in the promoter of *SmTAT1* and *SmDFR* as performed by Y1H (Fig. 6C-D). EMSA was performed to further verify whether SmbHLH60 is bound to the promoters of *SmTAT1* and *SmDFR*, and the pCold-His protein was used as a negative control. The band of the protein-probe complex was detected only in the presence of the SmbHLH60-His fusion protein, indicating that SmbHLH60 can bind to *SmTAT1* and *SmDFR* by the G-box in its promoter (Fig. 6E-F). These results revealed that *SmTAT1* and *SmDFR*, the target genes of SmbHLH60, were transcriptionally inhibited by SmbHLH60, which was consistent with the expression of *SmTAT1* and *SmDFR* in our qRT-PCR results.

SmbHLH60 interacts with SmMYC2 to form a heterodimer

Interestingly, the Y2H results showed that SmbHLH60 and SmMYC2 could interact directly (Fig. 7A). BiFC and GST pull-

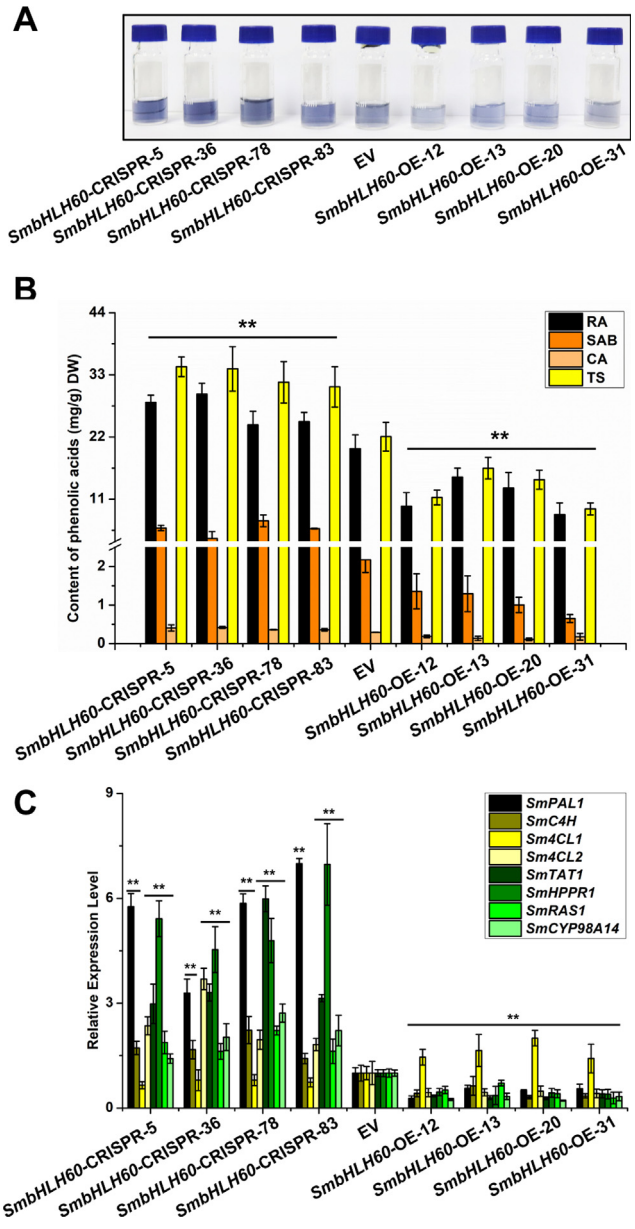

Fig. 4. SmbHLH60 negatively regulate biosynthetic genes and the production of phenolic acids (A). Color of total phenolic acids (TS) extracts of transgenic hairy roots. Folin-Phenol was used for staining of total phenolic acid extract. The shade of color represented the total content of phenolic acid. (B). Determination of total phenolic acid and three main phenolic acids including rosmarinic acid (RA), salvianolic acid B (SAB), caffeic acid (CA) by HPLC. The content determination of each hairy root line was repeated three times, and error bars represented the standard deviation of three biological replicates (*, $p < 0.05$; **, $p < 0.01$). (C). qRT-PCR was used to detect gene expressions of key enzymes in phenolic acid biosynthesis. Transcription levels of genes involved in phenolic acid biosynthesis were detected in *SmbHLH60*-CRISPR lines and *SmbHLH60*-OE lines respectively. All experiments were repeated three times, and error bars represented the standard deviation of three biological replicates (*, $p < 0.05$; **, $p < 0.01$).

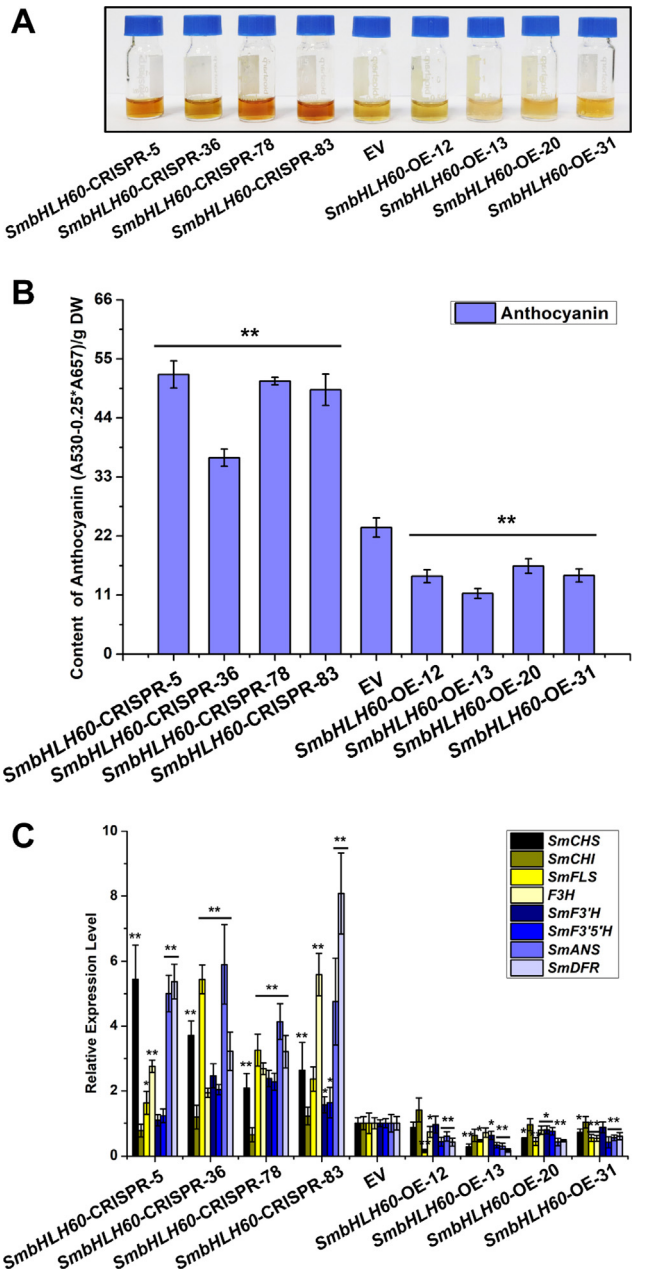

Fig. 5. *SmbHLH60* transgenic lines negatively regulate biosynthetic genes and total anthocyanins. (A). Color of anthocyanin extracts of transgenic hairy roots. The hydrochloric acid–methanol solution was used to extract total anthocyanins (v: v = 1: 99). The picture showed the product after the extraction of total anthocyanins. (B). Determination of total anthocyanins. The anthocyanin extract was mixed with an equal volume of chloroform and detected by a microplate reader (*, $p < 0.05$; **, $p < 0.01$). (C). qRT-PCR was used to detect gene expression of key enzymes in anthocyanin biosynthesis. All experiments were repeated three times, and error bars represented the standard deviation of three biological replicates (*, $p < 0.05$; **, $p < 0.01$).

down were performed to clarify the interaction between SmbHLH60 and SmMYC2. In BiFC assays, the peptides nYFP and cYFP were combined to excite fluorescence only when nYFP-SmbHLH60 and SmMYC2-cYFP combined, otherwise there was no fluorescence excitation (Fig. 7B). In the GST pull-down assay, the SmbHLH60-His fusion protein in the experimental group and input was detected through the His antibody, while GST protein and SmMYC2-GST fusion protein were detected through the GST antibody. SmbHLH60-His was incubated with SmMYC2-GST and GST, respectively. The result of the western blot (WB) assay found that the luminescence signal was only detected in the group where SmbHLH60-His and SmMYC2-GST were incubated together, while no band was detected in the group incubated with SmbHLH60-His and GST (Fig. 7C). These results indicated that an interaction existed between SmbHLH60 and SmMYC2.

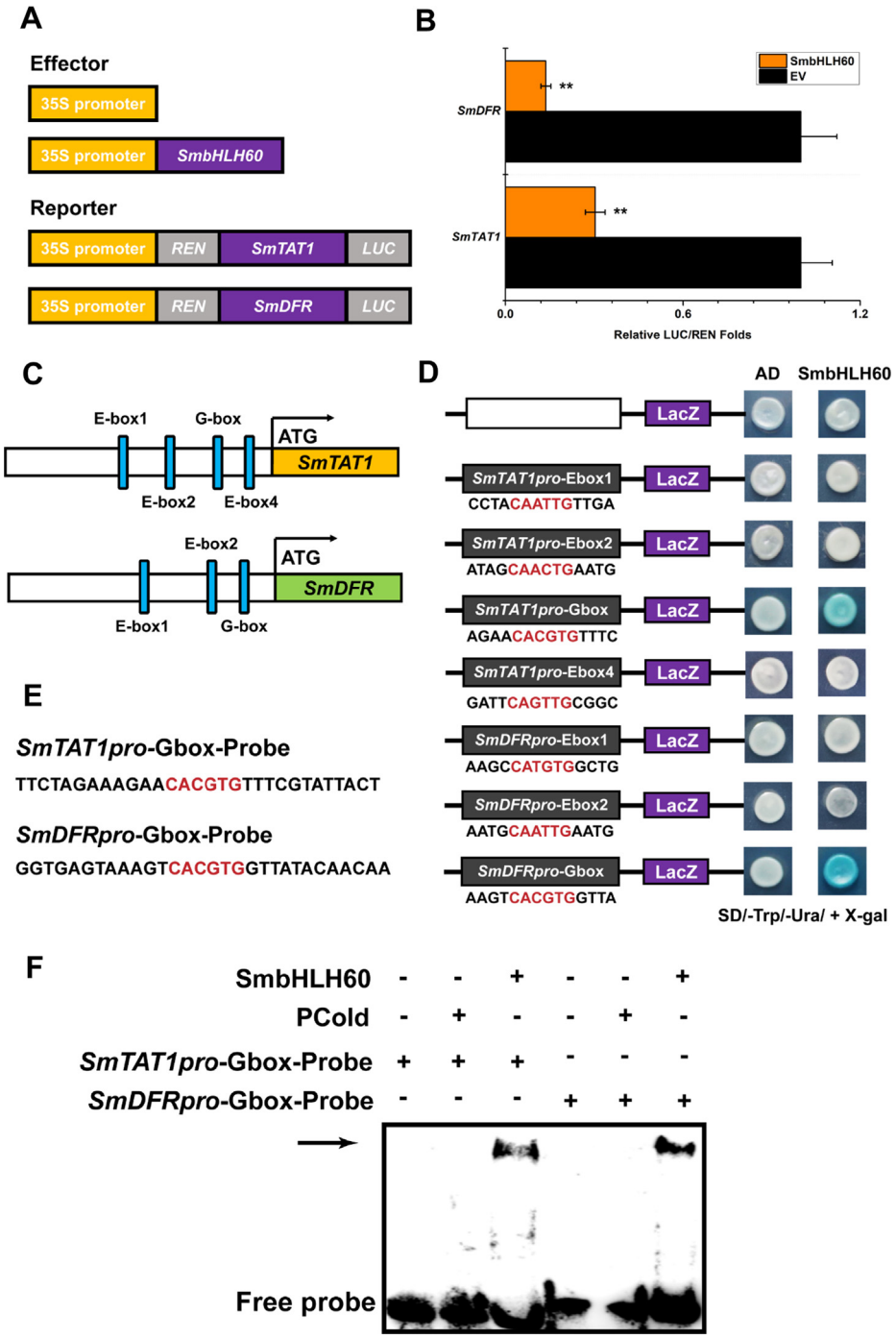

Fig. 6. SmbHLH60 can bind to the G-Box motif in the promoter region of *SmTAT1* and *SmDFR*. (A). Schematic diagram of constructs used in assays of transient transcriptional activity. (B). SmbHLH60 repressed promoters of *SmTAT1* and *SmDFR*, and the relative LUC activity was normalized to the *Renilla* (REN) luciferase. pGreen0800-*SmTAT1pro*-LUC and pGreen0800-*SmDFRpro*-LUC were co-injected with pHB-*SmbHLH60* respectively into tobacco epidermal cells for promoter activity determination. All experiments were carried out in three biological replicates and error bars represented the standard deviation of three biological replicates (*, $p < 0.05$; **, $p < 0.01$). (C). The positions of E/G-box elements in *SmTAT1pro and SmDFRpro* for Y1H and EMSA analysis. (D). The Y1H assays showed that SmbHLH60 bound to the G-box in the promoters of *SmTAT1* and *SmDFR*. Two vectors including pB42AD-*SmbHLH60* and pLacZ2u-E/G-box were transferred into EGY48 yeast, which was placed on a medium containing X-gal for selection. (E). Probe sequences used in the EMSA experiment including CACGTG conserved sequence. (F). Specific binding of SmbHLH60 to G-box in the promoters of *SmTAT1* and *SmDFR*. The third lane of the DNA-protein complex was detected, indicating that SmbHLH60 was directly bound to the probe containing the G-box element.

SmbHLH60 attenuates the transcriptional activation effect of SmMYC2 on SmTAT1 and SmDFR

The discovery that SmMYC2 and SmbHLH60 target the same genes provoked us to further investigate the molecular mechanism underlying this finding. Dual-LUC was performed to explore the effect of SmMYC2 and SmbHLH60 on *SmTAT1* and *SmDFR* transcription activation. Our results showed that SmMYC2 can activate *SmTAT1* and *SmDFR*, while SmbHLH60 can attenuate the expression of *SmTAT1* and *SmDFR* when SmMYC2 and SmbHLH60 existed alone. However, the transcriptional activation levels of *SmTAT1* and *SmDFR* were weakened when SmMYC2 and SmbHLH60 acted

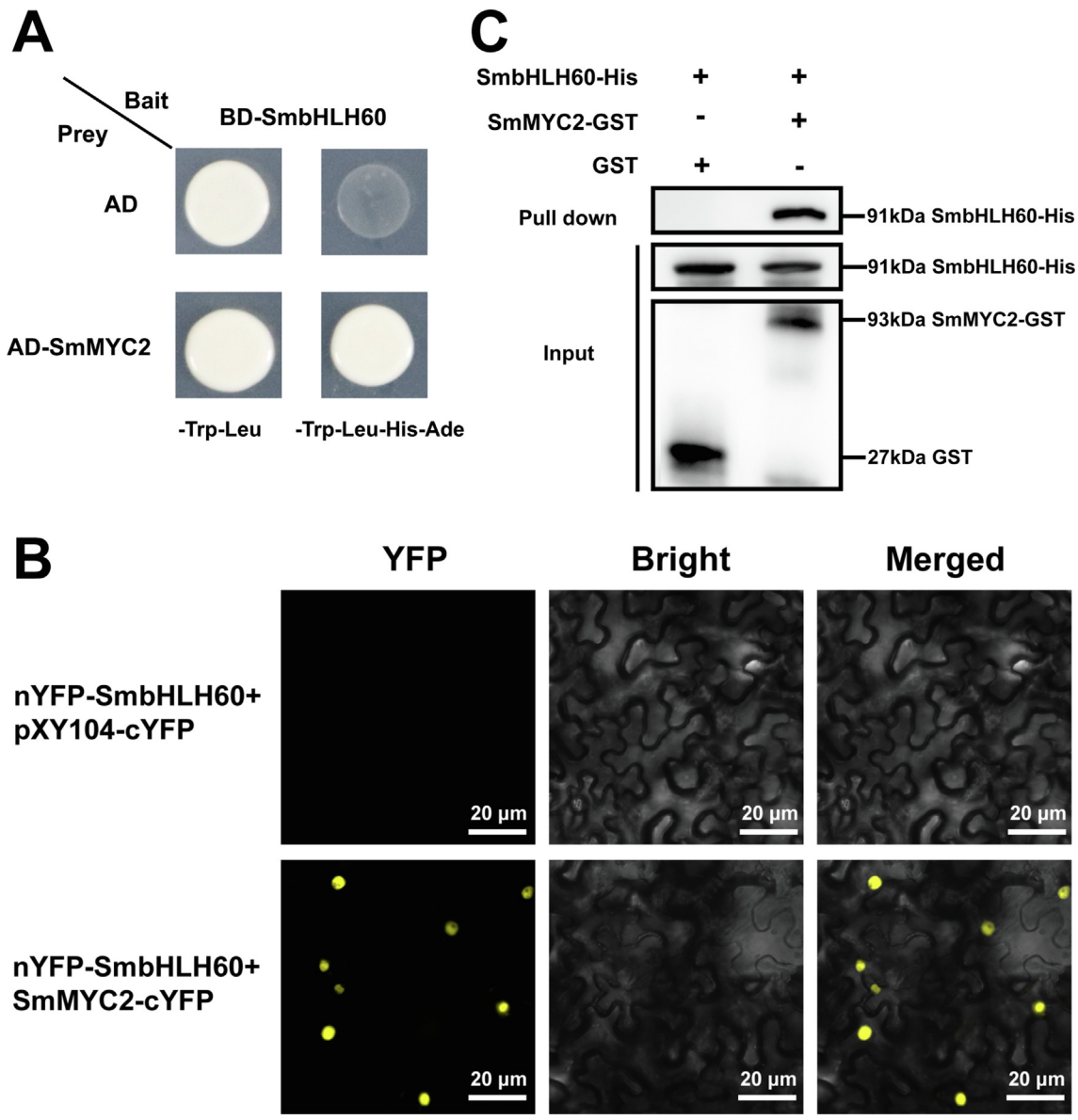

Fig. 7. SmbHLH60 interacted with SmMYC2 *in vitro* and *in vivo*. (A). Yeast-two-hybrid assay showed SmbHLH60 can interact with SmMYC2. The ORF of *SmMYC2* and *SmbHLH60* were connected to pGADT7 and pGBKT7, respectively. After AD-MYC2 and BD-SmbHLH60 were co-transformed, the yeast could grow normally on the SD/-Trp/-Leu/-His/-Ade medium. (B). Bimolecular fluorescent complementary assays to detect the interaction between SmbHLH60 and SmMYC2. The ORFs of *SmbHLH60* and *SmMYC2* were constructed on the pXY-106-nYFP vector and pXY-104-cYFP vector, respectively. Fluorescence could only be detected when nYFP-SmbHLH60 was combined with SmMYC2-cYFP, scale bar was 20 μm. (C). GST pull-down assay verified that SmbHLH60 could interact with SmMYC2. The fusion protein SmbHLH60-His and SmMYC2-GST were incubated together with magnetic beads. The final results were detected with the anti-His.

as the co-effector (Fig. 8A-B), suggesting that SmbHLH60 competed with SmMYC2 to bind to the promoters of *SmTAT1* and *SmDFR*. Especially, the SmMYC2-SmbHLH60 interaction did not affect the ability of SmbHLH60 to bind to the G-box probes of *SmTAT1pro* and *SmDFRpro* (Fig. 8C-D). To study the relationship between SmbHLH60 and SmMYC2, we detected the transcription level of SmMYC2 in SmbHLH60 transgenic plants. The transcription level of *SmMYC2* decreased in *SmbHLH60*-OE hairy roots, but increased in *SmbHLH60*-CRISPR hairy roots (Fig. 8E). Meanwhile, the expression of *SmbHLH60* was also detected in *SmMYC2*-OE lines, which showed that *SmbHLH60* was decreased (Fig. S9). These results indicated that SmbHLH60 and SmMYC2 function as antagonistic regulators of phenolic acid and anthocyanin biosynthesis by direct regulation of *SmTAT1* and *SmDFR*.

Discussion

MeJA has a central role in plant growth, development and adaptation to the environment [30,44]. In *S. miltiorrhiza*, MeJA promotes anthocyanin, tanshinones and phenolic acids accumulation [13,16,45,46]. Additionally, the effect of MeJA was also shown in the gene expression level [12,22]. However, the molecular mechanism(s) underlying the regulation of secondary metabolites, and more specifically for phenolic acids in *S. miltiorrhiza*, is still unknown. Generally, MeJA regulates secondary metabolic pathways through a cascade of transcription factors to regulate downstream key enzyme genes, which ultimately leads to changes in the accumulation of metabolites [30]. The molecular mechanism of how these key enzyme genes are regulated by the JA pathway is to be further analyzed.

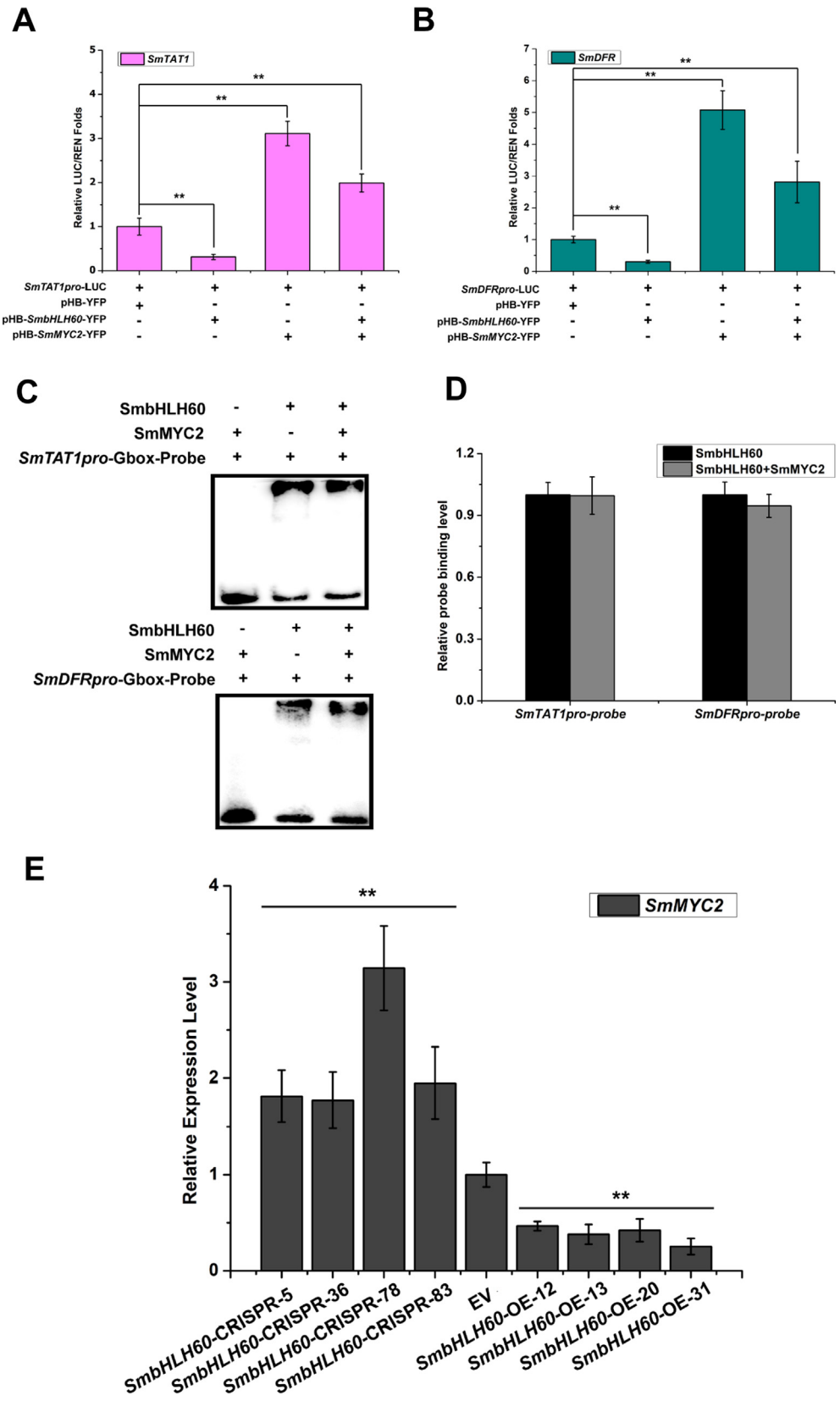
A
SmTAT1
Relative LUC/REN Folds
SmTAT1pro-LUC
pHB-YFP
pHB-SmbHLH60-YFP
pHB-SmMYC2-YFP
B
SmDFR
Relative LUC/REN Folds
SmDFRpro-LUC
pHB-YFP
pHB-SmbHLH60-YFP
pHB-SmMYC2-YFP
C
SmbHLH60
SmMYC2
SmTAT1pro-Gbox-Probe
SmbHLH60
SmMYC2
SmDFRpro-Gbox-Probe
D
SmbHLH60
SmbHLH60+SmMYC2
Relative probe binding level
SmTAT1pro-probe
SmDFRpro-probe
E
SmMYC2
Relative Expression Level
SmbHLH60-CRISPR-5
SmbHLH60-CRISPR-36
SmbHLH60-CRISPR-78
SmbHLH60-CRISPR-83
EV
SmbHLH60-OE-12
SmbHLH60-OE-13
SmbHLH60-OE-20
SmbHLH60-OE-31

Fig. 8. Competition between SmbHLH60 and SmMYC2 attenuates a promoter-dependent transcriptional activation of *SmTAT1* and *SmDFR*. (A). Effectors SmbHLH60 and SmMYC2 were co-transformed with reporters *SmTAT1pro*-LUC. We mixed pHB-SmbHLH60 with pHB-MYC2 and injected it with pGreen0800-*SmTAT1*-LUC into tobacco epidermal cells and tested the results. (B). Effectors SmbHLH60 and SmMYC2 were co-transformed with reporters *SmDFRpro*-LUC. pHB-*SmbHLH60* and pHB-*MYC2* were mixed, which were injected with pGreen0800-*SmDFR*-LUC into tobacco epidermal cells and detected the results. All data were means of three biological replicates with error bars indicating standard deviation (*, $p < 0.05$; **, $p < 0.01$). (C). EMSA was used to detect whether the SmbHLH60-SmMYC2 interaction would affect the ability of SmbHLH60 to bind to the *SmTAT1* and *SmDFR* promoters by EMSA. SmMYC2 and SmbHLH60 were separately or mixed and then incubated with the biotin-labeled probes *SmTAT1pro* and *SmDFRpro* for EMSA. (D). The gray value of the bound probe was statistically used to detect whether the SmMYC2-SmbHLH60 interaction would affect the binding of SmbHLH60 to the *SmTAT1pro* and *SmDFRpro*. All gray values were means of three biological replicates with error bars indicating standard deviation (*, $p < 0.05$; **, $p < 0.01$). (E). qRT-PCR was performed to detect the transcription level of *SmMYC2* in *SmbHLH60* transgenic plants. The relative quantitative analysis method ($2^{-\Delta\Delta CT}$) was used to calculate the relative gene expression, and *SmActin* was used as the internal reference gene. All experiments were repeated three times, and error bars represented the standard deviation of three biological replicates (*, $p < 0.05$; **, $p < 0.01$).

The bHLH transcription factor, MYC2, was shown to act as a core regulator in the MeJA signaling pathway [44]. In a previous report, it was found that SmMYC2, the core transcription factor for JA signaling, is a positive regulator of *SmPAL1*, *SmTAT1* and *SmCYP98A14* (37, 41). However, the mechanism by which SmMYC2 regulates JA-mediated phenolic acid biosynthesis remains unclear. In this study, a novel interactor of SmMYC2 that functions as a negative regulator in phenolic acid biosynthesis. Moreover, SmbHLH60 binds to and represses the promoters of *SmTAT1* and *SmDFR*. SmbHLH60 and SmMYC2 antagonistically interact to regulate *SmTAT1* and *SmDFR* expression. Therefore, we propose that plants regulate the biosynthesis of phenolic acid and anthocyanin mediated by the bHLH complex in *S. miltiorrhiza* through the JA signaling pathway.

SmbHLH60 may be involved in MeJA-mediated phenolic acid biosynthesis as a negative regulator

MeJA has been proven to be an effective inducer that can cause the accumulation of phenolic acid [13,16,23]. To explore the molecular mechanism of phenolic acid accumulation in *S. miltiorrhiza* which is regulated by MeJA, the MeJA-mediated transcriptome data in *S. miltiorrhiza* was analyzed. We identified 89 bHLH transcription factors that are down-regulated by MeJA, of which *SmbHLH60* was one of the most significantly down-regulated genes (Fig. 1A). SmbHLH92 have been characterized to negatively regulate phenolic acid biosynthesis [8]. Interestingly, *SmbHLH92* showed reduced transcription levels in MeJA-mediated RNA-seq data while *SmMCY2* increased in RNA-seq data (Fig. S5). The expression pattern of *SmbHLH60* after MeJA treatment is consistent with *SmbHLH92*. These results suggest that SmbHLH60 may be a negative regulator.

In previous research, SmMYB1 has been proved to promote phenolic acid biosynthesis show a consistent expression pattern with the expression of genes in the biosynthetic pathway of phenolic acid increased significantly after MeJA treatment [3]. However, *SmbHLH60* showed an expression pattern opposite to key enzyme genes including *SmPAL1*, *SmC4H*, *SmTAT*, *SmHPPR*, *SmRAS* and *SmCYP98A14*. These results indicated that SmbHLH60 may hold a negative regulatory role in the MeJA-mediated biosynthesis of phenolic acid. Therefore, we decided to focus on deciphering the role of this gene in regulating phenolic acid biosynthesis.

SmbHLH60 negatively regulates the biosynthesis of phenolic acid in S. Miltiorrhiza by repressing SmTAT1

It was found that total phenolic acids in hairy roots increased significantly after *SmbHLH60* was knocked out, which was 1.48 times that of the control line. Conversely , the content of phenolic acids decreased by 40% compared with the control in the *SmbHLH60*-OE lines (Fig. 4B). These results showed SmbHLH60 exhibited an opposite effect to SmMYC2. Several important genes of the phenolic acid biosynthesis pathway, including *SmPAL1*, *SmC4H*, *Sm4CL2*, *SmTAT1*, *SmHPPR1*, *SmRAS1*, and *SmCYP98A14*, were suppressed in the presence of *SmbHLH60*. Meanwhile, the expression of these genes increased when *SmbHLH60* was knocked out (Fig. 4C). The reason for the detection of *Sm4CL2* expression is that previous studies have shown that *Sm4CL2* may play a more important role in synthesizing phenolic acids [13,47,48]. Among them, the expression of *SmPAL1*, *SmTAT1* and *SmHPPR1* increased significantly in the *SmbHLH60*-CRISPR lines. RA and SAB levels were significantly decreased in accordance with the downregulation of *SmPAL1* confirming the importance of *SmPAL1* in phenolic acid biosynthesis [13]. Overexpression of *SmTAT1* led to a significant increase of the RA and SAB content than the wild type [13,16,49]. Furthermore, the expression of *SmTAT1* and *SmHPPR1* was associated with the biosynthesis of RA and SAB after being treated with MeJA or other treatments, suggesting that the tyrosine conversion is a rate-limiting step in the biosynthesis of phenolic acids [13,16,50,51]. These results support the hypothesis that SmbHLH60 acts as a negative regulator of the biosynthesis of phenolic acids.

We detected 7 possible candidate target genes in phenolic acid biosynthesis of SmbHLH60 by dual-LUC (Fig. 6B, S7). Our results showed that SmbHLH60 transcriptionally repressed *SmPAL1*, *SmTAT1* and *SmRAS1*, which indicated that *SmPAL1*, *SmTAT1* and *SmRAS1* might be the target genes of SmbHLH60. Furthermore, Y1H and EMSA results showed that SmbHLH60 bound to the G-box of *SmTAT1pro* (Fig. 6D, F). Interestingly, SmbHLH60 did not bind to the E-box of *SmTAT1pro* (Fig. 6D). *SmTAT1* is the first committing enzymatic step in the tyrosine pathway [16,46]. It is worth noting that our investigation demonstrated that SmbHLH60 regulates *SmTAT1* expression by direct binding to its G-box (CACGTG) promoter region. These results revealed that SmbHLH60 bound to the promoter of *SmTAT1* and suppress its expression to reduce phenolic acid biosynthesis in *S. miltiorrhiza*.

SmbHLH60 represses the expression of SmDFR to negatively regulate anthocyanin biosynthesis

The total anthocyanins were extracted and it was found that the color of the *SmbHLH60* transgenic hairy root extract was significantly different from that of the control (Fig. 5A). Therefore, we are curious whether SmbHLH60 directly caused the difference in the color of anthocyanin extracts. As a result, total anthocyanin content in the knockout line reached twice that of the control line. Conversely, in hairy roots overexpressing *SmbHLH60*, the total anthocyanin content was only 59% of the control line (Fig. 5B). The expression of key genes in anthocyanin biosynthesis, including *SmCHS*, *SmFLS*, *SmF3H*, *SmF3′H*, *SmF3′5′H*, *SmANS* and *SmDFR* were decreased to varying degrees in the *SmbHLH60-OE* lines. Especially, *SmFLS*, *SmANS* and *SmDFR* are significantly suppressed. On the contrary, these genes showed an upward trend in *SmbHLH60*-CRISPR lines (Fig. 5C). The expressions of *SmCHI*, *SmANS* and *SmDFR* were significantly up-regulated in the *SmbHLH60*-CRISPR lines. These results indicated that SmbHLH60 negatively regulates biosynthesis not only phenolic acids but also anthocyanins.

Dual-LUC assays verified that SmbHLH60 can transcriptionally repress the expression of *SmDFR*, but it has no regulatory effect on other several anthocyanin genes (*SmF3H*, *SmCHS*, *SmANS*) (Fig. 8B, S7). Subsequently, we wonder whether SmbHLH60 binds to the G-box binding site in the *SmDFR* promoter. The dihydroflavonol reductase (DRF) is an important key enzyme in the pathway of anthocyanin biosynthesis [3,52,53]. For example, the biosynthesis of anthocyanins in apples is regulated by DFR activity [52]. DFR catalyzes a significant step in the biosynthesis of anthocyanins and proanthocyanidins by reducing dihydroflavonols to anthocyanins (53). Besides, *SmDFR* has been identified in *S. miltiorrhiza* [22] and few reports that TFs directly regulate anthocyanin biosynthesis have been reported. Our results found that SmbHLH60 directly bound to the G-box but not E-box of the *SmDFR* promoter. As we predicted, SmbHLH60 directly regulated the expression of *SmDFR* and reduced total anthocyanins in hairy roots.

In addition to phenolic acid and anthocyanin, we also found that SmbHLH60 may also negatively affect the accumulation of tanshinones. However, the molecular mechanism requires further research in the future (Fig. S8).

SmbHLH60 and SmMYC2 antagonistic function in a bHLH heterodimer to regulate the biosynthesis of phenolic acids and anthocyanins

bHLH-type TFs usually function as homodimer or heterodimer [30]. Although SmbHLH53 has been reported to interact with SmMYC2, the mechanism by which they regulate phenolic acid biosynthesis remains unclear [14]. Different types of transcription factors can also form complexes to regulate downstream target genes. For instance, SmMYB1 has been reported to form a complex with SmMYC2 to regulate *SmCYP98A14* and to induce phenolic acid accumulation [3]. In this study, we identified that the SmbHLH60 interacted with SmMYC2 through the Y2H assays (Fig. 7A). BiFC and GST pull-down assays also verified the interaction between SmMYC2 and SmbHLH60 (Fig. 7B-C). These results revealed that SmbHLH60 directly interacted with SmMYC2 to form a heterodimer.

SmMYC2 has been reported to bind to *SmTAT1* and promote its transcriptional activation [37]. Interestingly, we found that SmbHLH60 bound to and transcriptionally repressed *SmTAT1* expression (Fig. 6B-C). SmbHLH60 repressed the expression of *SmDFR* in contrast to the results that SmMYC2 promoted the transcriptional activation of *SmDFR* as was demonstrated by dual-LUC assay (Fig. 8A-B). Y1H results showed that SmMYC2 was bound to the *SmTAT1pro* and *SmDFRpro*, which indicated that *SmTAT1* and *SmDFR* were target genes for SmMYC2 (Fig. S10A). Thus, we postulate that SmbHLH60 and SmMYC2 antagonistically regulate *SmTAT1* and *SmDFR* by binding different elements of *SmTAT1* and *SmDFR*. In order to verify our hypothesis, we performed dual-LUC assays by co-injecting SmMYC2 and SmbHLH60 into *N. benthamiana* leaves with *SmTAT1* and *SmDFR*, respectively. The promotion effects of SmMYC2 on *SmTAT1* and *SmDRF* were impaired when SmbHLH60 was present (Fig. 8A-B). Interestingly, we found that the SmMYC2-SmbHLH60 interaction did not affect the ability of

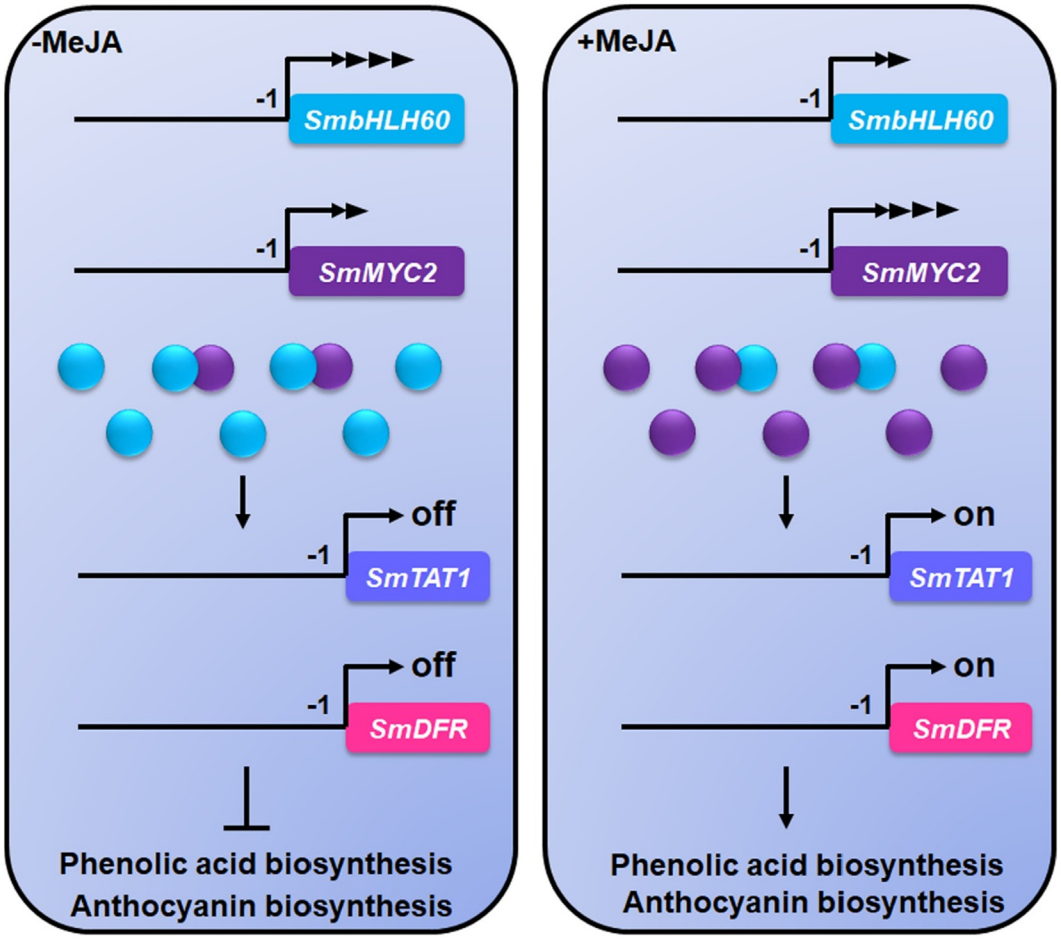

Fig. 9. Proposed mechanism for the regulation of phenolic acids biosynthesis by SmbHLH60 in *S. miltiorrhiza*. SmbHLH60 and SmMYC2 antagonized the regulation of phenolic acid biosynthesis. Under the treatment of MeJA, *SmbHLH60* was suppressed and the expression of *SmMYC2* was increased, which led to the increase in the expressions of *SmTAT1* and *SmDFR*, resulting in the production of phenolic acid and anthocyanin increased ultimately.

SmbHLH60 to bind to the *SmTAT1* and *SmDFR* promoters (Fig. 8C-D). Y1H results also showed that the binding sites of SmbHLH60 and SmMYC2 to *SmTAT1pro* and *SmDFRpro* were different (Fig. S10B). This result also implied that the binding sites of SmMYC2 and SmbHLH60 were not the same although both bound to the promoter of *SmTAT1*. Furthermore, we found that the expression of *SmMYC2* was decreased in *SmbHLH60*-OE hairy roots, but increased in *SmbHLH60*-CRISPR hairy roots (Fig. 8E). In the contrast, *SmbHLH60* was repressed in *SmMYC2*-OE lines (Fig. S9). These results indicate that SmbHLH60 and SmMYC2 antagonistically control phenolic acid and anthocyanin biosynthesis by competing with the promoters of *SmTAT1* and *SmDFR*. Furthermore, we found that SmbHLH60 interacted with SmJAZ-1like, SmJAZ8 and SmJAZ9 (Fig. S11A-B). Based on these results, we speculate that SmbHLH60 may form an inhibitory complex with JAZs to participate in phenolic acid biosynthesis. However, how the SmJAZs, SmbHLH60 and SmMYC2 work together to regulate phenolic acid and anthocyanin biosynthesis still needs more exploration in the future.

A new model - SmbHLH60 as a negative regulator for the production of phenolic acids and anthocyanins

We proposed a new hypothetical working model for the SmbHLH60 and SmMYC2 antagonistic regulation of phenolic acid and anthocyanin biosynthesis mediated by MeJA in *S. miltiorrhiza* (Fig. 9). In the absence of MeJA, *SmTAT1* and *SmDFR* are repressed by the SmbHLH60. Meanwhile, SmbHLH60 and SmMYC2 form a heterodimer, which inhibited the transcriptional activation of SmMYC2 on *SmTAT1* and *SmDFR*. However, MeJA leads to a decrease in the expression of *SmbHLH60* while increasing the expression of *SmMYC2*. Furthermore, these changes in expression result in a reduction of the inhibitory effect of *SmTAT1* and *SmDFR* and enhancement of the transcriptional activation by SmMYC2. Finally, this complexed bHLH-JA dependent regulation results in increased production of phenolic acids and anthocyanins in *S. miltiorrhiza*. In summary, our discovery provides novel insights into the regulatory mechanism of bHLH-type TFs as heterodimers in the regulation of secondary metabolites which lays a foundation for further research of MeJA-mediated biosynthesis in plants.

Conclusions

In this study, a bHLH negatively regulated by MeJA was identified and characterized, named SmbHLH60. SmbHLH60 regulates phenolic acid and anthocyanin biosynthesis in *S. miltiorrhiza* roots. The expression of *SmbHLH60* was negatively correlated to the phenolic acid and anthocyanin concentrations as was shown in the OE and knockout lines. Key biosynthetic genes involved in the anthocyanin and phenolic acid production were up-regulated in the *SmbHLH60*-CRISPR lines and down-regulated in the *SmbHLH60*-OE lines. Furthermore, we have elucidated the molecular machinery in which SmbHLH60 regulates secondary metabolites. SmbHLH60 can directly bind *SmTAT1* and *SmDFR* and repress their expression through their promoters. A SmbHLH60-SmMYC2 dimer takes part in the regulation of phenolic acid and anthocyanin biosynthesis in *S. miltiorrhiza*. These results shed new light on the role of bHLH transcription factors in the biosynthesis of phenolic acids and anthocyanins through heterodimers in *S. miltiorrhiza*, and provide new insights for the analysis of the MeJA-mediated regulation network of secondary metabolites.

Compliance with Ethics Requirements

This research has fully complied with research ethics.

CRediT authorship contribution statement

Shucan Liu: Conceptualization, Validation, Formal analysis, Investigation, Writing – original draft, Visualization, Writing – review & editing. **Yao Wang:** Conceptualization, Validation, Writing – review & editing. **Min Shi:** Formal analysis, Validation, Writing – review & editing. **Itay Maoz:** Writing – review & editing. **Xiankui Gao:** Formal analysis, Investigation. **Meihong Sun:** Investigation. **Tingpan Yuan:** Validation, Investigation. **Kunlun Li:** Investigation, Formal analysis. **Wei Zhou:** Writing – review & editing. **Xinhong Guo:** Writing – review & editing, Supervision. **Guoyin Kai:** Conceptualization, Resources, Writing – review & editing, Supervision, Project administration, Funding acquisition.

Declaration of Competing Interest

The authors declare that they have no known competing financial interests or personal relationships that could have appeared to influence the work reported in this paper.

Acknowledgment

This work was supported by the National Natural Science Fund of China [82073963, 81522049, 31571735]; The Major Science and Technology Projects of Breeding New Varieties of Agriculture in Zhejiang Province [2021C02074]; Zhejiang Provincial Ten Thousand Program for Leading Talents of Science and Technology Innovation [2018R52050]; Zhejiang Provincial Program for the Cultivation of High-Level Innovative Health Talents; The Opening Project of Zhejiang Provincial Preponderant and Characteristic Subject of Key University (Traditional Chinese Pharmacology), Zhejiang Chinese Medical University [ZYAOX2018009; ZYAOXYB2019002]. The Research Project of Zhejiang Chinese Medical University [2021JKZDZC06].

Appendix A. Supplementary data

Supplementary data to this article can be found online at https://doi.org/10.1016/j.jare.2022.02.005.

References

[1] Hao XL, Pu ZQ, Cao G, You DW, Zhou Y, Deng CP, et al. Tanshinone and salvianolic acid biosynthesis are regulated by SmMYB98 in *Salvia miltiorrhiza* hairy roots. J Adv Res 2020;23:1–12. doi: https://doi.org/10.1016/j.jare.2020.01.012.

[2] Huang Q, Sun MH, Yuan TP, Wang Y, Shi M, Lu SJ, et al. The AP2/ERF transcription factor SmERF1L1 regulates the biosynthesis of tanshinones and phenolic acids in *Salvia miltiorrhiza*. Food Chem 2019;274:368–75. doi: https://doi.org/10.1016/j.foodchem.2018.08.119.

[3] Zhou W, Shi M, Deng CP, Lu SJ, Huang FF, Wang Y, et al. The methyl jasmonate-responsive transcription factor SmMYB1 promotes phenolic acid biosynthesis in *Salvia miltiorrhiza*. Hortic Res 2021;8(1):10. doi: https://doi.org/10.1038/s41438-020-00443-5.

[4] Zhou W, Li S, Maoz I, Wang Q, Xu M, Feng Y, et al. SmJRB1 positively regulates the accumulation of phenolic acid in *Salvia miltiorrhiza*. Ind Crops Prod 2021;164:113417. doi: https://doi.org/10.1016/j.indcrop.2021.113417.

[5] Ren J, Fu L, Nile SH, Zhang J, Kai GY. *Salvia miltiorrhiza* in treating cardiovascular diseases: a review on its pharmacological and clinical applications. Front Pharmacol 2019;10:753. doi: https://doi.org/10.3389/fphar.2019.00753.

[6] Deng CP, Shi M, Fu R, Zhang Y, Wang Q, Zhou Y, et al. ABA-responsive transcription factor bZIP1 is involved in modulating biosynthesis of phenolic acids and tanshinones in *Salvia miltiorrhiza*. J Exp Bot 2020;71(19):5948–62. doi: https://doi.org/10.1093/jxb/eraa295.

[7] Meim XD, Cao YF, Che YY, Li J, Shang ZP, Zhao WJ, et al. Danshen: a phytochemical and pharmacological overview. Chin J Nat Med 2019;17(1):59–80. doi: https://doi.org/10.1016/S1875-5364(19)30010-X.

[8] Zhang JH, Lv HZ, Liu WJ, Ji AJ, Zhang X, Song JY, et al. bHLH transcription factor SmbHLH92 negatively regulates biosynthesis of phenolic acids and tanshinones in *Salvia miltiorrhiza*. Chin Herb Med 2020;12(3):237–46. doi: https://doi.org/10.1016/j.chmed.2020.04.001.

[9] Xiao Z, Liu W, Mu YP, Zhang H, Wang XN, Zhao CQ, et al. Pharmacological effects of salvianolic acid B against oxidative damage. Front Pharmacol 2020;11(3). doi: https://doi.org/10.3389/fphar.2020.572373.
[10] Wang B, Sun W, Li QS, Li Y, Luo MH, Song JY, et al. Genome-wide identification of phenolic acid biosynthetic genes in *Salvia miltiorrhiza*. Planta 2015;241 (3):711–25. doi: https://doi.org/10.1007/s00425-014-2212-1.
[11] Huang WP, Zhang Y, Song J, Zhao LJ, Wang ZZ. De novo transcriptome sequencing in *Salvia miltiorrhiza* to identify genes involved in the biosynthesis of active ingredients. Genomics 2011;98(4):272–9. doi: https://doi.org/10.1016/j.ygeno.2011.03.012.
[12] Deng CP, Wang Y, Huang FF, Lu SJ, Zhao LM, Ma XY, et al. SmMYB2 promotes salvianolic acid biosynthesis in the medicinal herb *Salvia miltiorrhiza*. J Integr Plant Biol 2020;62(11):1688–702. doi: https://doi.org/10.1111/jipb.12943.
[13] Ma XH, Ma Y, Tang JF, He YL, Liu YC, Ma XJ, et al. The biosynthetic pathways of tanshinones and phenolic acids in *Salvia miltiorrhiza*. Molecules 2015;20 (9):16235–54. doi: https://doi.org/10.3390/molecules200916235.
[14] Peng JJ, Wu YC, Wang SQ, Niu JF, Cao XY. SmbHLH53 is relevant to jasmonate signaling and plays dual roles in regulating the genes for enzymes in the pathway for salvianolic acid B biosynthesis in *Salvia miltiorrhiza*. Gene 2020;756:144920. doi: https://doi.org/10.1016/j.gene.2020.144920.
[15] Fu R, Shi M, Deng CP, Zhang Y, Zhang XC, Wang Y, et al. Improved phenolic acid content and bioactivities of *Salvia miltiorrhiza* hairy roots by genetic manipulation of RAS and CYP98A14. Food Chem 2020;331:127365. doi: https://doi.org/10.1016/j.foodchem.2020.127365.
[16] Shi M, Huang FF, Deng CP, Wang Y, Kai GY. Bioactivities, biosynthesis and biotechnological production of phenolic acids in *Salvia miltiorrhiza*. Crit Rev Food Sci Nutr 2019;59(6):953–64. doi: https://doi.org/10.1080/10408398.2018.1474170.
[17] Song J, Wang ZZ. RNAi-mediated suppression of the phenylalanine ammonia-lyase gene in *Salvia miltiorrhiza* causes abnormal phenotypes and a reduction in rosmarinic acid biosynthesis. J Plant Res 2011;124(1):183–92. doi: https://doi.org/10.1007/s10265-010-0350-5.
[18] Wang GQ, Chen JF, Yi B, Tan HX, Zhang L, Chen WS. HPPR encodes the hydroxyphenylpyruvate reductase required for the biosynthesis of hydrophilic phenolic acids in *Salvia miltiorrhiza*. Chin J Nat Med 2017;15(12):917–27. doi: https://doi.org/10.1016/S1875-5364(18)30008-6.
[19] Di P, Zhang L, Chen JF, Tan HX, Xiao Y, Dong X, et al. ^{13}C tracer reveals phenolic acids biosynthesis in hairy root cultures of *Salvia miltiorrhiza*. ACS Chem Biol 2013;8(7):1537–48. doi: https://doi.org/10.1021/cb3006962.
[20] An JP, Xu RR, Liu X, Zhang JC, Wang XF, You CX, et al. Jasmonate induces anthocyanin and proanthocyanidin biosynthesis in apple by mediating the JAZ1-TRB1-MYB9 complex. Plant J 2021;106(5):1414–30. doi: https://doi.org/10.1111/tpj.15245.
[21] Liu YF, Ma KX, Qi YW, Lv GW, Ren XL, Liu ZD, et al. Transcriptional regulation of anthocyanin synthesis by MYB-bHLH-WDR complexes in Kiwifruit (*Actinidia chinensis*). J Agric Food Chem 2021;69(12):3677–91. doi: https://doi.org/10.1021/acs.jafc.0c07037.
[22] Deng YX, Li CL, Li HQ, Lu SF. Identification and characterization of flavonoid biosynthetic enzyme genes in *Salvia miltiorrhiza (Lamiaceae)*. Molecules 2018;23(6):1467. doi: https://doi.org/10.3390/molecules23061467.
[23] Liang ZS, Ma YN, Xu T, Cui BM, Liu Y, Guo ZX, et al. Effects of abscisic acid, gibberellin, ethylene and their interactions on production of phenolic acids in *Salvia miltiorrhiza Bunge* hairy roots. PLoS ONE 2013;8(9):e72806. doi: https://doi.org/10.1371/journal.pone.0072806.
[24] Dong JE, Wan GW, Liang ZS. Accumulation of salicylic acid-induced phenolic compounds and raised activities of secondary metabolic and antioxidative enzymes in *Salvia miltiorrhiza* cell culture. J Biotechnol 2010;148(2–3):99–104. doi: https://doi.org/10.1016/j.jbiotec.2010.05.009.
[25] Guo HB, Dang XL, Dong JE. Hydrogen peroxide and nitric oxide are involved in salicylic acid-induced salvianolic acid B production in *Salvia miltiorrhiza* cell cultures. Molecules 2014;19(5):5913–24. doi: https://doi.org/10.3390/molecules19055913.
[26] Wang YC, Liu WJ, Jiang HY, Mao ZL, Wang N, Jiang SH, et al. The R2R3-MYB transcription factor MdMYB24-like is involved in methyl jasmonate-induced anthocyanin biosynthesis in apple. Plant Physiol Biochem 2019;139:273–82. doi: https://doi.org/10.1016/j.plaphy.2019.03.031.
[27] Chini A, Gimenez-Ibanez S, Goossens A, Solano R. Redundancy and specificity in jasmonate signaling. Curr Opin Plant Biol 2016;33:147–56. doi: https://doi.org/10.1016/j.pbi.2016.07.005.
[28] Zhou ML, Memelink J. Jasmonate-responsive transcription factors regulating plant secondary metabolism. Biotechnol Adv 2016;34(4):441–9. doi: https://doi.org/10.1016/j.biotechadv.2016.02.004.
[29] De Geyter N, Gholami A, Goormachtig S, Goossens A. Transcriptional machineries in jasmonate-elicited plant secondary metabolism. Trends Plant Sci 2012;17(6):349–59. doi: https://doi.org/10.1016/j.tplants.2012.03.001.
[30] Goossens JJ, Mertens J, Goossens A. Role and functioning of bHLH transcription factors in jasmonate signalling. J Exp Bot 2017;68(6):1333–47. doi: https://doi.org/10.1093/jxb/erw440.
[31] Ezer D, Shepherd SJK, Brestovitsky A, Dickinson P, Cortijo S, Charoensawan V, et al. The G-Box transcriptional regulatory code in *Arabidopsis*. Plant Physiol 2017;175(2):628–40. doi: https://doi.org/10.1104/pp.17.01086.
[32] Fernandez-Calvo P, Chini A, Fernandez-Barbero G, Chico JM, Gimenez-Ibanez S, Geerinck J, et al. The *Arabidopsis* bHLH transcription factors MYC3 and MYC4 are targets of JAZ repressors and act additively with MYC2 in the activation of jasmonate responses. Plant Cell 2011;23(2):701–15. doi: https://doi.org/10.1105/tpc.110.080788.
[33] Zhang X, Luo MH, Xu ZC, Zhu YJ, Ji AJ, Song JY, et al. Genome-wide characterisation and analysis of bHLH transcription factors related to tanshinone biosynthesis in *Salvia miltiorrhiza*. Sci Rep 2015;5:11244. doi: https://doi.org/10.1038/srep11244.
[34] Zhang CL, Xing BC, Yang DF, Ren M, Guo H, Yang SS, et al. SmbHLH3 acts as a transcription repressor for both phenolic acids and tanshinone biosynthesis in *Salvia miltiorrhiza* hairy roots. Phytochemistry 2020;169:112183. doi: https://doi.org/10.1016/j.phytochem.2019.112183.
[35] Xing BC, Liang LJ, Liu L, Hou ZN, Yang DF, Yan KJ, et al. Overexpression of *SmbHLH148* induced biosynthesis of tanshinones as well as phenolic acids in *Salvia miltiorrhiza* hairy roots. Plant Cell Rep 2018;37(12):1681–92. doi: https://doi.org/10.1007/s00299-018-2339-9.
[36] Xing BC, Yang DF, Yu HZ, Zhang BX, Yan KJ, Zhang XM, et al. Overexpression of *SmbHLH10* enhances tanshinones biosynthesis in *Salvia miltiorrhiza* hairy roots. Plant Sci 2018;276:229–38. doi: https://doi.org/10.1016/j.plantsci.2018.07.016.
[37] Du TZ, Niu JF, Su J, Li SS, Guo XR, Li L, et al. SmbHLH37 functions antagonistically with SmMYC2 in regulating jasmonate-mediated biosynthesis of phenolic acids in *Salvia miltiorrhiza*. Front Plant Sci 2018;9. doi: https://doi.org/10.3389/fpls.2018.01720.
[38] Wu YC, Zhang Y, Li L, Guo XR, Wang B, Cao XY, et al. AtPAP1 interacts with and activates SmbHLH51, a positive regulator to phenolic acids biosynthesis in *Salvia miltiorrhiza*. Front Plant Sci 2018;9:1687. doi: https://doi.org/10.3389/fpls.2018.01687.
[39] Shen Q, Lu X, Yan TX, Fu XQ, Lv ZY, Zhang FY, et al. The jasmonate-responsive AaMYC2 transcription factor positively regulates artemisinin biosynthesis in *Artemisia annua*. New Phytol 2016;210(4):1269–81. doi: https://doi.org/10.1111/nph.13874.
[40] Zhang HT, Hedhili S, Montiel G, Zhang YX, Chatel G, Pré M, et al. The basic helix-loop-helix transcription factor CrMYC2 controls the jasmonate-responsive expression of the ORCA genes that regulate alkaloid biosynthesis in *Catharanthus roseus*. Plant J 2011;67(1):61–71. doi: https://doi.org/10.1111/j.1365-313X.2011.04575.x.
[41] Yang N, Zhou WP, Su J, Wang XF, Li L, Wang LR, et al. Overexpression of *SmMYC2* increases the production of phenolic acids in *Salvia miltiorrhiza*. Front Plant Sci 2017;8. doi: https://doi.org/10.3389/fpls.2017.01804.
[42] Sun MH, Shi M, Wang Y, Huang Q, Yuan TP, Wang Q, et al. The biosynthesis of phenolic acids is positively regulated by the JA-responsive transcription factor ERF115 in *Salvia miltiorrhiza*. J Exp Bot 2019;70(1):243–54. doi: https://doi.org/10.1093/jxb/ery349.
[43] Hung FY, Lai YC, Wang J, Feng YR, Shih YH, Chen JH, et al. The Arabidopsis histone demethylase JMJ28 regulates CONSTANS by interacting with FBH transcription factors. Plant Cell 2021;33(4):1196–211. doi: https://doi.org/10.1093/plcell/koab014.
[44] Shu P, Li ZY, Min DD, Zhang XH, Ai W, Li JZ, et al. CRISPR/Cas9-mediated SlMYC2 mutagenesis adverse to tomato plant growth and MeJA-induced fruit resistance to *Botrytis cinerea*. J Agric Food Chem 2020;68(20):5529–38. doi: https://doi.org/10.1021/acs.jafc.9b08069.
[45] Xiao Y, Gao SH, Di P, Chen JF, Chen WS, Zhang L. Methyl jasmonate dramatically enhances the accumulation of phenolic acids in *Salvia miltiorrhiza* hairy root cultures. Physiol Plant 2009;137(1):1–9. doi: https://doi.org/10.1111/j.1399-3054.2009.01257.x.
[46] Xing BC, Yang DF, Liu L, Han RL, Sun YF, Liang ZS. Phenolic acid production is more effectively enhanced than tanshinone production by methyl jasmonate in *Salvia miltiorrhiza* hairy roots. Plant Cell Tiss Org 2018;134(1):119–29. doi: https://doi.org/10.1007/s11240-018-1405-x.
[47] Jin XQ, Chen ZW, Tan RH, Zhao SJ, Hu ZB. Isolation and functional analysis of 4-coumarate:coenzyme A ligase gene promoters from *Salvia miltiorrhiza*. Biol Plantarum 2012;56(2):261–8. doi: https://doi.org/10.1007/s10535-011-0231-3.
[48] Zhao SJ, Hu ZB, Liu D, Leung FCC. Two divergent members of 4-coumarate: coenzyme A ligase from *Salvia miltiorrhiza Bunge*. J Integr Plant Biol 2006;48 (11):1355–64. doi: https://doi.org/10.1111/j.1744-7909.2006.00302.x.
[49] Xiao Y, Zhang L, Gao SH, Saechao S, Di P, Chen JF, et al. The c4h, tat, hppr and hppd genes prompted engineering of rosmarinic acid biosynthetic pathway in *Salvia miltiorrhiza* hairy root cultures. PLoS ONE 2011;6(12):e29713. doi: https://doi.org/10.1371/journal.pone.0029713.
[50] Zhang SC, Yan Y, Wang BQ, Liang ZS, Liu Y, Liu FH, et al. Selective responses of enzymes in the two parallel pathways of rosmarinic acid biosynthetic pathway to elicitors in *Salvia miltiorrhiza* hairy root cultures. J Biosci Bioeng 2014;117 (5):645–51. doi: https://doi.org/10.1016/j.jbiosc.2013.10.013.
[51] Yan Q, Shi M, Ng J, Wu JY. Elicitor-induced rosmarinic acid accumulation and secondary metabolism enzyme activities in *Salvia miltiorrhiza* hairy roots. Plant Sci 2006;170(4):853–8.
[52] Chen WF, Zhang MX, Zhang GJ, Li PM, Ma FW. Differential regulation of anthocyanin synthesis in apple peel under different sunlight intensities. Int J Mol Sci 2019;20(23):6060. doi: https://doi.org/10.3390/ijms20236060.
[53] Lim SH, Park B, Kim DH, Park S, Yang JH, Jung J-A, et al. Cloning and functional characterization of dihydroflavonol 4-reductase gene involved in anthocyanin biosynthesis of *Chrysanthemum*. Int J Mol Sci 2020;21(21):7960. doi: https://doi.org/10.3390/ijms21217960.